Journal of Virology

Effects of Potyvirus Effective Population Size in Inoculated Leaves on Viral Accumulation and the Onset of Symptoms

Mark P. Zwart, José-Antonio Daròs and Santiago F. Elena
J. Virol. **2012, 86(18):9737. DOI: 10.1128/JVI.00909-12.**
Published Ahead of Print 27 June 2012.

JVI Journals.ASM.org

Effects of *Potyvirus* Effective Population Size in Inoculated Leaves on Viral Accumulation and the Onset of Symptoms

Mark P. Zwart,[a] José-Antonio Daròs,[a] and Santiago F. Elena[a,b]

Instituto de Biología Molecular y Celular de Plantas, Consejo Superior de Investigaciones Científicas-UPV, València, Spain,[a] and The Santa Fe Institute, Santa Fe, New Mexico, USA[b]

Effective population size (N_e) is a key parameter for understanding evolutionary processes, but it is generally not considered in epidemiological studies or in studying infections of individual hosts. Whether N_e has an effect on the onset of symptoms and viral accumulation in *Tobacco etch virus* (TEV) infection of *Nicotiana tabacum* plants is considered here. Using mixtures of TEV variants carrying fluorescent markers, the dose dependence of N_e was confirmed, and the inoculation procedure was found to be the main source of variation in these experiments. Whereas the onset of symptoms was independent of N_e, there was less and more variable accumulation at 6 days postinoculation for small N_e values ($N_e < 5$). The observed variation in accumulation was not heritable, however, suggesting that this variation was not due to the fixation of deleterious mutations in the small founder populations. On the other hand, virus-induced fluorescence and accumulation in the inoculated leaf were strongly N_e dependent. Systemic accumulation was independent of N_e, although removal of the inoculated leaf led to a small reduction in systemic accumulation for small N_e values. For whole plants, N_e-dependent effects on accumulation were no longer observed at 9 days postinoculation. Therefore, the effects of N_e on accumulation are due mainly to limited expansion in the inoculated leaf and are transient. In this system, N_e-dependent effects will be strongest at low doses and early in infection. We conclude that N_e can have implications for epidemiology and infection at the individual host level, beyond determining the rate of mixed-genotype infection.

Effective population size (N_e) is a concept introduced by Wright (in 1931) to better understand how the number of individuals within a population affects the outcome of evolution (38). N_e gives an approximation of the number of breeding individuals in an idealized population or, in the case of viruses, the number of transmitting individuals (8, 25). This number indicates the strength with which genetic drift will act on the virus population (38), as well as the frequency at which mixed-genotype infections will occur (40). Mixed-genotype infections are relevant for understanding evolution because they are a prerequisite for recombination between different viral strains (10). Census size (N), on the other hand, is the observed number of individuals in the population at a given moment. Whereas N values tend to be huge for viruses, N_e values can be very small under certain conditions (i.e., low pathogen doses or low levels of host susceptibility) (15).

Many studies have shown that N_e can be very small for plant viruses by considering the transition from initial to systemic infection (9, 14, 22, 29) or vector-borne transmission (1, 5, 14, 24). It was recently shown that small N_e values also occur during infection following mechanical inoculation and that dose-response relationships, the number and distribution of primary infection foci, and the frequency of mixed-genotype infections conform to independent action hypothesis (IAH) model predictions (39). The IAH model assumes that each virion has a nonzero probability of infection and that virions infect the host such that the action of each virion is independent of that of other virions (2). Alternative models of infection can incorporate dependent action (DA) (i.e., dose-dependent effects on the probability of infection for each virion) or heterogeneous host susceptibility (HHS) (i.e., differences in infection probability per virion over hosts) (28). Although there is support for the IAH model for some monopartite viruses (39, 40), the model can be rejected *a priori* for multipartite viruses that encapsidate the different genome segments separately. In these cases, there will be complementation between the different virion types, and hence a dependent action model would be more appropriate. It must also be stressed that the models of infection considered here describe conspecific virus populations and that the terms "genotypes" and "mixed-genotype infection" refer to virus variants that are identical except for a neutral marker (40). Therefore, both the models and the experiments have no bearing on the occurrence of a variety of interactions between distinct genotypes. In the field, interactions between virus genotypes can be complex and highly relevant (e.g., see references 12 and 27). IAH leads to a dose-dependent N_e; N_e is then simply the product of dose and the probability of infection (39). Although N_e has been quantified for a number of plant viruses, the relationship between N_e and N has not, to our knowledge, been described quantitatively for viral infection of a complex multicellular host.

The concept of N_e is rooted in evolutionary biology, and indeed, it has been shown to be extremely important for understanding evolutionary processes (25, 38). On the other hand, N_e is usually not considered an important parameter on relatively short time scales, such as those often studied in epidemiology. For modeling of the epidemiology of microparasites, host organisms are usually considered within the SIR (susceptible, infectious, and removed) framework or variations thereof, including the SEIR (susceptible, exposed, infectious, and removed) model with a latent period of infection. This widely used and immensely successful approach (18) therefore focuses on how many host organisms are in a particular state, not on attributes of the virus population (19).

Received 12 April 2012 **Accepted** 22 June 2012
Published ahead of print 27 June 2012
Address correspondence to Mark P. Zwart, marzwa@upvnet.upv.es.

doi:10.1128/JVI.00909-12

For plant pathogens, classical epidemiological models have also considered the amounts of uninfected (i.e., susceptible), latently infected (i.e., exposed), and infectious tissue (17, 35), again focusing on host states. Recently, it was suggested that integration of the between-host and within-host levels and the approaches used to study them will increase our understanding of infectious disease dynamics (13, 23). Whether the inclusion of the concept of N_e could lead to a better understanding of the epidemiology of plant viruses is therefore considered here.

A similar question could be asked concerning even shorter time scales: is N_e a useful and necessary concept for describing the infection process in individual plants? In experiments comparing different plant genotypes, the viral dose (3) or mRNA inoculum (21) is often held constant. Even though dose can be used to predict N_e under the IAH model (39), the two are not equivalent. If it is assumed that dose is fixed, then N_e will not be the same in all hosts, even when there is no experimental variation (i.e., no variation in dose and a homogeneous host population). When the IAH model with a fixed probability of infection over hosts is supported, N_e follows a Poisson distribution (39, 40). For example, for a Poisson-distributed N_e with a mean of 5, it would be expected that ~25% of the hosts would be infected with ≤ 2 or ≥ 8 individuals.

There is one important case in which N_e is highly relevant for processes at both the epidemiological and individual plant scales, i.e., the occurrence of mixed-genotype infections. N_e is an important determinant of whether mixed-genotype infections will occur, together with the frequencies and infection probabilities of different viral genotypes in the virus population. Mixed-genotype infections in turn can have important implications for infectious disease dynamics on different spatiotemporal scales (12, 27, 30, 31, 33). However, besides this obvious case, the question of whether N_e merits attention on relatively short temporal scales remains.

In this study, the relationship between N_e and the infection process in individual plants was investigated to explore whether N_e has further implications. It was previously reported that N_e is predicted by the IAH model and therefore dose dependent for *Tobacco etch virus* (TEV; genus *Potyvirus*, family *Potyviridae*) infection of tobacco plants (*Nicotiana tabacum* L.), allowing for simple estimates of N_e by considering the number of primary infection foci (39). This approach was exploited to look for effects on the onset of symptoms and viral accumulation. Virus-induced symptoms may play a role in attracting vectors (16, 32) and can therefore influence horizontal transmission of viruses; viral accumulation will affect the probability of a vector becoming viruliferous (26).

MATERIALS AND METHODS

Inoculation experiments with mixtures of TEV-GFP and TEV-mCherry. To generate virion stocks, RNAs were transcribed *in vitro* for pMTEV-GFP and pMTEV-mCherry (39) as described previously (6). *N. tabacum* cv. Xanthi was used for all experiments. Plants were infected with 5 μg RNA in the third true leaf, and the symptomatic systemically infected tissue was collected at 9 days postinoculation (dpi) and used for purification of virions (6). Virions were resuspended in 100 μl of 0.05 M borate buffer (pH 8.0, with 5 mM EDTA) with 20% glycerol. Virion concentration was determined by reverse transcription-quantitative PCR (RT-qPCR), using *in vitro*-synthesized *Turnip mosaic virus* (TuMV) RNA as an internal control (39).

One-to-one mixtures of TEV-GFP and TEV-mCherry virions were then made, and 5-μl samples of serial dilutions of these mixtures were used to rub inoculate 25-day-old *N. tabacum* plants (39). Plants were kept in a greenhouse until inoculation and then transferred to a growth chamber and kept at 24°C. All plants used for experiments were selected stringently for having the same size and synchronous development. Green fluorescent protein (GFP) and mCherry fluorescence was observed using a Leica MZ16F stereomicroscope with a 0.5× objective and GFP2 and DSR filters (Leica), respectively. Foci of primary infection in the inoculated leaf were counted at 3 dpi, and systemic infection was determined at 6 dpi. Those plants with virus-induced fluorescence in systemic tissues at 6 dpi were considered infected plants, unless otherwise noted. Whether TEV symptoms were present was also determined at 6 dpi, unless otherwise noted. For the time course experiment, the occurrence of TEV symptoms was recorded at all times of tissue collection (3, 6, 9, and 12 dpi). For experiments to determine the median time until onset of symptoms (ST_{50}), symptoms were recorded daily from the moment of inoculation until all plants had developed symptoms.

Two replicates of the main experiment were performed. The total number of plants challenged with each virion dilution was 20 (1:10, 1:30, and 1:90), 25 (1:270), 35 (1:810), 75 (1:2,430), or 30 (nonvirus control). Larger numbers of plants were inoculated for the higher virion dilutions in order to have sufficient infected plants for subsequent analysis. For the time course experiments, 30 plants were infected with a 1:10 virion dilution, 75 plants were infected with a 1:270 virion dilution, and 15 nonvirus controls were taken. For the ST_{50} experiments, 30 plants were infected with a 1:10 virion dilution, 50 plants were infected with a 1:270 virion dilution, and 10 plants were taken as mock-inoculated controls.

RT-qPCR for viral accumulation. Plants were collected at 6 dpi by removing all of the aerial tissue, although multiple time points were used for the time course assay (3, 6, 9, and 12 dpi). Moreover, for experiments on accumulation in the inoculated leaf, the inoculated leaf and the remaining aerial tissue were collected and stored separately. The collected tissue was weighed and then stored at −80°C. Total RNA was extracted from 100 mg of tissue by use of an Invitrap Spin plant RNA miniprep kit (Stratec Molecular). One-step RT-qPCR using specific primers for the coat protein (forward primer, 5′-TTGGTCTTGATGGCAACGTG-3′; and reverse primer, 5′-TGTGCCGTTCAGTGTCTTCCT-3′) was performed with a Primescript RT-PCR kit II (TaKaRa) according to the manufacturer's instructions, using a Prism 7500 sequence analyzer (Applied Biosystems). Data were then analyzed with Prism 7500 software, version 2.0.4 (Applied Biosystems).

Statistical analysis. All statistical analyses were performed in R, version 2.10.1 (The R Foundation, Austria, Vienna), unless otherwise noted. The dose-focus relationship was analyzed as previously reported (39). Briefly, focus data (λ) were transformed with the equation $y = \ln(\lambda + 1)$, and the equation $y = \ln(\rho d + 1)$, where d is the dose and ρ is the average infection probability, was then fitted by nonlinear regression (SPSS 16.0; SPSS Inc., Chicago, IL). The $\ln(\lambda + 1)$ transformation was used because some leaves were uninfected.

The DA model of dose-response relationships (28) is $I = 1 - e^{-\rho d^{\phi}}$, where I is the fraction of systemically infected plants, d is the virion dose, and ϕ determines the effect of dose on the rate of infection. The IAH model of infection is similar to the DA model, but ϕ is fixed to 1 so there are no dose-dependent effects on the actual infection probability per virion (28). In the DA model, when ϕ is >1, there is synergism between virions (dose-response curve is steeper than that predicted by IAH), while when ϕ is <1, there is antagonism (dose-response curve is shallower than that predicted by IAH). The dose-response model incorporating HHS (4) is as follows:

$$I = \left(\frac{1}{1 + d\rho v}\right)^{\frac{1}{v}}$$

where v determines the variability in host susceptibility and is a nonnegative real number. Increases in v represent increasing HHS, with zero indicating no variation in host susceptibility. These three models (IAH,

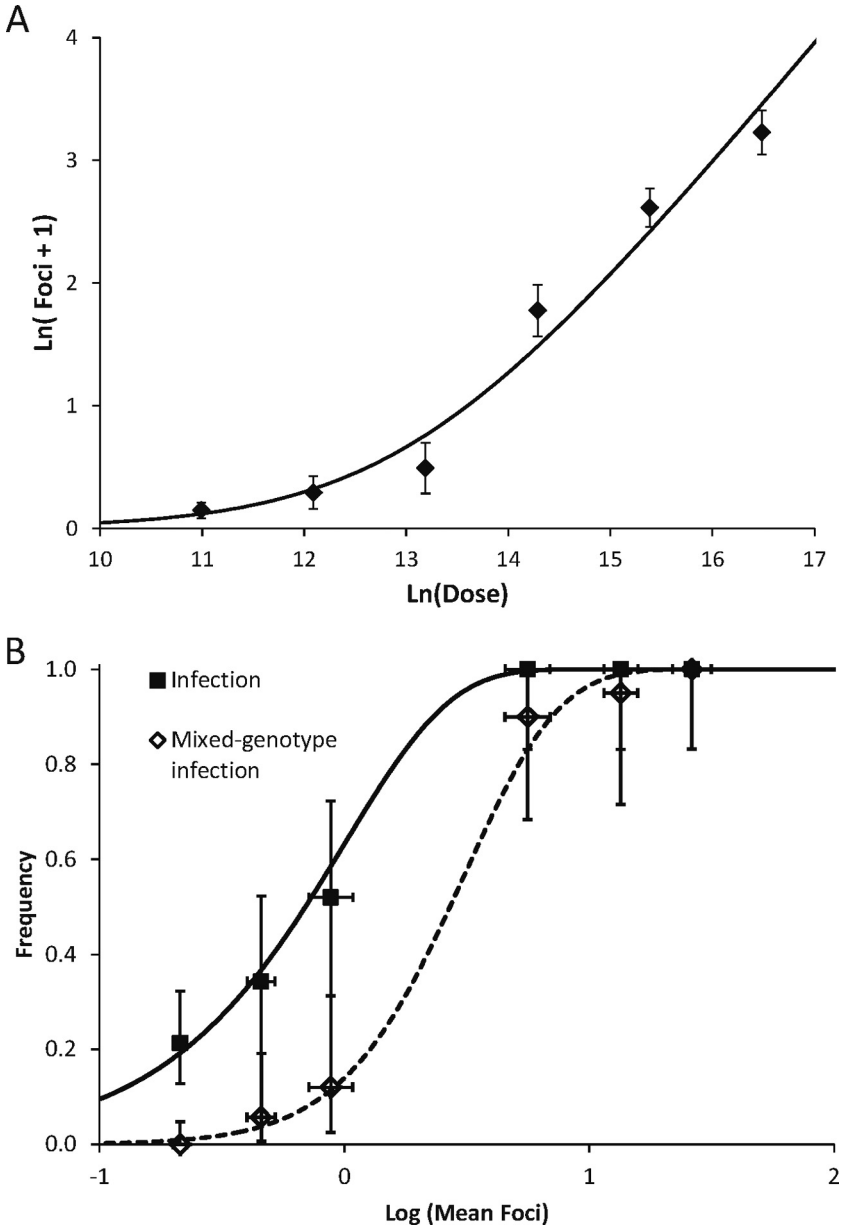

FIG 1 Comparison of IAH model predictions and data. Comparisons are shown for IAH model predictions and data for the dose-focus relationship (A) and for rates of infection and mixed-genotype infection (B). In panel A, the ln-transformed dose is plotted on the abscissa, and the ln-transformed number of foci plus 1 is plotted on the ordinate. In panel B, the value for log mean foci is plotted on the abscissa, while the frequency of infection (squares and solid line) or mixed-genotype infection (diamonds and dotted line) is plotted on the ordinate. For both panels, error bars represent 95% confidence intervals. None of the data points in panel B are significantly different from model predictions (Table 3).

DA, and HHS) were fit to the data by use of a maximum likelihood approach in which likelihoods were calculated using binomial probabilities. Binomial probabilities could be used because the data were analyzed as infected/noninfected and symptomatic/nonsymptomatic. Grid searches were first performed over a large parameter space, followed by searches over consecutively smaller spaces. This approach ensured that the solution found was both precise and global.

A geometric model was fitted to the N_e accumulation relationship. As N_e increases by 1, viral accumulation (A) becomes $A_{N_e} + 1 = A_{N_e} + ck^{N_e}$, where c is a constant scaling the rate of change and determining whether N_e increases (positive values) or decreases (negative values) and k is a constant that determines whether the increase or decrease remains the same ($k = 1$) or becomes larger ($k > 1$) or smaller ($k < 1$) as N_e increases. The solution for A_{N_e} is as follows:

$$A_{N_e} = \begin{cases} A_0 + \dfrac{c(1 - k^{N_e})}{1 - k} & \text{for } k \neq 1 \\ A_0 + cN_e & \text{for } k = 1 \end{cases}$$

This model was fit to the data by use of nonlinear regression (SPSS 16.0).

For the accumulation data from the time course experiments, the following logistic model was fitted: $n_t = \dfrac{n_0\kappa}{n_0 + (\kappa - n_0)e^{-r_0 t}}$, where n_t is viral accumulation at time t, n_0 is viral accumulation at time zero, κ is the

TABLE 1 Variance in mean number of foci of primary infection[a]

Dilution	Virion dose	Mean no. of foci	Variance	z	P
1:10	1.44×10^7	26.25	113.67	1.217	0.103
1:30	4.81×10^6	13.45	21.00	0.719	0.680
1:90	1.60×10^6	5.60	10.88	0.936	0.345
1:270	5.34×10^5	0.88	1.11	0.326	1
1:810	1.78×10^5	0.46	0.43	0.067	1
1:2,430	5.94×10^4	0.21	0.17	0.184	1

[a] The dilution of purified virions used to inoculate plants and the estimated virion dose, estimated by the number of RNA molecules measured by RT-qPCR, are given. The mean number of foci of primary infection for both TEV-GFP and TEV-mCherry in an inoculated leaf is given. Variance is the calculated variance of the mean number of foci of primary infection. For a Poisson distribution, the mean is equal to the variance. Whether this holds true for the data was tested by means of a one-sample Kolmogorov-Smirnoff (KS) test, where z is the KS test statistic and P is its significance. No test results are significantly different from model predictions, although the variance deviates more strongly from predictions at higher doses.

carrying capacity, and r_0 is the initial growth rate. Note that according to the definitions used here, n_0 is equivalent to N_e. The different symbols are used, though, to distinguish between estimates made by counting foci of primary infection (N_e) and estimates made by fitting the logistic model to RT-qPCR data from the time course (n_0).

RESULTS AND DISCUSSION

Infection process conforms to IAH model predictions. The IAH model is supported for TEV infection of *N. tabacum* (39). In this study, *N. tabacum* plants were inoculated with different doses of a 1:1 mixture of viruses tagged with fluorescent markers (TEV-GFP and TEV-mCherry), as previously described (39). The number of foci of primary infection was quantified using a stereomicroscope at 3 dpi, and whether systemic infection had occurred was determined at 6 dpi. All infection parameters conformed to IAH model predictions, including (i) the number of primary infection foci (Fig. 1A), (ii) the distribution of primary infection foci (Table 1), (iii) the dose-response relationship of infection (Fig. 1B and 2; Table 2), and (iv) the rate of mixed-genotype systemic infection (Fig. 1B; Table 3). Model selection was used to determine the most suitable dose-response infection model, and the IAH model was compared to more complex models incorporating a dose-dependent probability of infection (DA) or differences in host susceptibility to the virus (HHS) (see Materials and Methods). Both the DA and HHS models predicted dose-infection relationships slightly shallower than those shown by the data. The DA model predicted antagonistic interactions between virions ($\phi < 1$), and the HHS model predicted the occurrence of differences in host susceptibility ($\nu > 0$). There were, however, no appreciable differences in support for the different models (Table 2), and hence the IAH model was not rejected. Furthermore, in only one case was a plant observed in which exclusion of one genotype (TEV-mCherry) by systemic infection by the other (TEV-GFP) occurred. In total, only 1 of 291 infected plants showed this phenomenon, and this observation had a statistically insignificant difference (test of equal proportions; $P = 0.576$) from previous observations (3/275 plants) (39). The data are therefore in agreement with IAH predictions, as shown in a previous study (39), allowing inferences to be made about N_e and how it changes with dose.

Sources of variation in the infection process. Infection parameters were not significantly different from IAH model predictions. Nevertheless, the distribution of primary infection foci tended toward a higher variance than that predicted at high doses (Table 1), and the dose-response curve appeared to be slightly shallower, as also indicated by estimated parameter values for the dose-response relationship ($\phi < 1$ or $\nu > 0$) (Table 2). Both trends have been observed before in this experimental system (39), as well as for other plant viruses (11, 20). Moreover, these trends appear to be quite general, since they also appear in other experimental systems (4, 28, 36, 40), where it must be noted that a higher variance in the distribution of founders is equivalent to an increase in mixed-genotype infection frequency (36). Thus, although deviations from the model were not in themselves suffi-

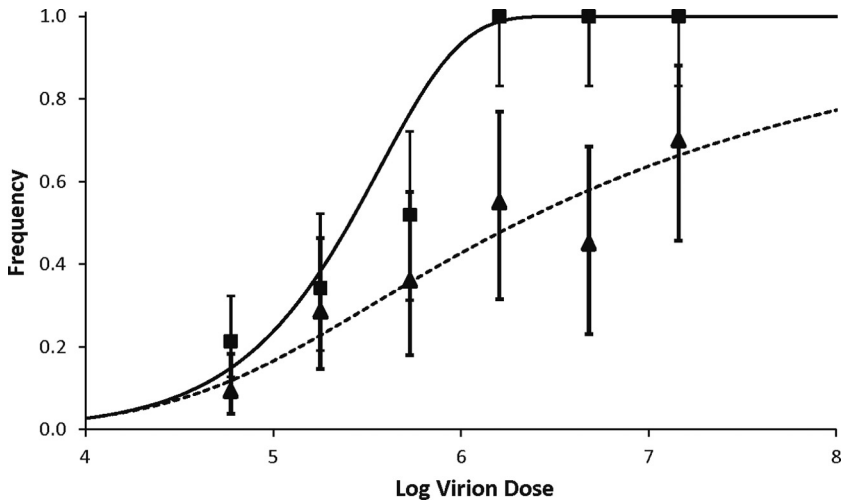

FIG 2 Dose-symptomatology relationship at 6 dpi. The log virion dose is plotted on the abscissa, and the frequency of symptomatology or infection at 6 dpi is plotted on the ordinate. The symptomatology data are given by triangles (mean ± 95% confidence interval), whereas squares represent infection data for comparison. The HHS model was plotted for dose-symptomatology data (dotted line), as this model gave the lowest Akaike weight (Table 1). However, the HHS model does not have appreciably more support than the DA model. For the dose-infection curve, the IAH model was plotted, as this is the simplest model and neither of the other models has appreciably more support (Table 2). Note that the dose-symptomatology curve is much shallower than the dose-response curve and that the frequency of symptomatic plants is considerably lower than the frequency of infected plants.

TABLE 2 Fitting of three dose-response models to dose-infection and dose-symptomatology data[a]

Type of data	Model	No. of model parameters	NLL	AIC	ΔAIC	AW	ρ	ϕ or *v* value
Infection	DA	2	9.10	22.20		0.523	3.69×10^{-4}	ϕ = 0.78
	IAH	1	10.55	23.10	0.90	0.333	2.33×10^{-6}	
	HHS	2	10.39	24.78	2.58	0.144	2.71×10^{-6}	*v* = 0.24
Symptomatology	HHS	2	12.19	28.39		0.794	2.95×10^{-6}	*v* = 4.91
	DA	2	13.55	31.09	2.70	0.206	2.71×10^{-3}	ϕ = 0.37
	IAH	1	48.43	98.87	70.48	0.000	2.33×10^{-7}	

[a] Models fitted to the data are the independent action hypothesis (IAH), dependent action (DA), and heterogeneous host susceptibility (HHS) models. NLL, negative log likelihood; AIC, Akaike information criterion; ΔAIC, difference in AIC compared to the best-supported model, which is given on top for both infection and symptomatology data. The infection probability (ρ) is given for all models, and fitted parameters ϕ and *v* are given where applicable. The difference between the DA and IAH models is only marginal for the infection data (ΔAIC < 2), while the HHS model gives a somewhat better fit than the DA model for symptomatology data (ΔAIC > 2). For the DA model, ϕ is <1 in both cases, which is representative of a shallow dose-response curve and antagonistic interactions between virions.

cient to reject IAH or to support an alternative model of infection, the generality of these subtle discrepancies gives good grounds for investigating the underlying mechanisms. Heterogeneity in host susceptibility has been implicated in departures from the IAH model; this model can reasonably account for dose-response and mixed-genotype infection data if the probability of infection is allowed to vary over hosts (4, 36).

To test what possible source of minor variation could occur in these experiments, both halves of leaves of *N. tabacum* plants were inoculated with TEV-GFP, and the number of primary infection foci was scored 3 days later. If the variation was at the between-plant level, one would expect to see a correlation between the numbers of foci on half leaves of the same plant. On the other hand, if variation occurred at the within-plant level—which would strongly implicate the inoculation procedure as the source of variation—one would expect to see no correlation between the numbers of foci on half leaves. No correlation between numbers of foci on half leaves was found (Table 4), suggesting that the main source of extra variation in the number of foci was the inoculation procedure itself.

No effects of dose and N_e on the occurrence or onset of TEV symptoms. Whether TEV symptoms were present in challenged plants was determined on day 6. Plants were classified as being symptomatic or nonsymptomatic. The frequency of symptoms clearly increased with dose (Fig. 2). On the other hand, a Jonckheere-Terpstra (JT) test for trend showed that when only infected plants were considered, the frequency of symptoms did not increase with dose ($P = 0.820$). The number of foci of primary infection is a good approximation of N_e (39). Whether there is a relationship between N_e and the frequency of symptoms in infected plants could therefore be tested, and this also gave a nonsignificant result (JT test; $P = 0.782$). Therefore, if a plant is infected, the probability that it will develop symptoms by 6 dpi appears to be independent of dose or N_e. Different dose-response models were then fitted to the dose-symptomatology data (see Materials and Methods). Although the IAH model was not well supported in this case, support for the alternative models—DA and HHS—was almost equal, with only marginally more support for the HHS model (Table 2). Hence, the dose-response models do not help to discriminate between these two mechanisms that could underlie the development of symptoms.

Viral accumulation was measured at 6 dpi by RT-qPCR amplification of the capsid protein gene (CP gene) in 10 randomly selected samples for each dose. It was found that viral accumulation was significantly higher in symptomatic plants than in nonsymptomatic plants (one-tailed Mann-Whitney test; $P = 0.033$). It therefore appears as if infected plants have a probability of developing symptoms by day 6 which is independent of virion dose and N_e but is affected by viral accumulation. This result is relevant from an epidemiological perspective because symptoms can affect vector-borne transmission (16, 32), and it therefore supports the exclusion of N_e from epidemiological models.

In the initial experiment, symptomatology was recorded only at 6 dpi. No dose- or N_e-dependent effects were observed, and it

TABLE 3 Comparison of data and model predictions for rates of infection and mixed-genotype infection[a]

Dilution	Virion dose	Mean no. of foci	Infections			Mixed-genotype infections		
			I_{obs} (no. of infected plants/no. of inoculated plants)	I_{pred}	*P* value	$P_{obs}(R \cap G)$ (no. of infected plants/no. of inoculated plants)	$P_{pred}(R \cap G)$	*P* value
1:10	1.44×10^7	26.25	1 (20/20)	1	1	1 (20/20)	1	1
1:30	4.81×10^6	13.45	1 (20/20)	1	1	0.950 (19/20)	0.990	0.182
1:90	1.60×10^6	5.60	1 (20/20)	0.996	1	0.900 (18/20)	0.831	0.559
1:270	5.34×10^5	0.88	0.520 (13/25)	0.585	0.546	0.120 (3/25)	0.114	0.759
1:810	1.78×10^5	0.46	0.343 (12/35)	0.369	0.862	0.057 (2/35)	0.038	0.386
1:2,430	5.94×10^4	0.21	0.213 (16/75)	0.189	0.557	0 (0/75)	0.009	1

[a] Dilution is the dilution of the virus stock used to inoculate plants, and virion dose is the number of virions per inoculated plant estimated by RT-qPCR. The observed rates of infection (I_{obs}) and mixed-genotype infection [$P_{obs}(R \cap G)$] were compared to model predictions [I_{pred} and $P_{pred}(R \cap G)$, respectively]. *P* values are significance values from a binomial test comparing data and model predictions. None of the observed infection or mixed-genotype infection rates are significantly different from model predictions.

TABLE 4 Correlation of numbers of foci on separately inoculated half leaves[a]

Dilution	Virion dose	Mean no. of foci per half leaf ± SD		Pearson correlation	*P* value
		Left	Right		
1:10	2.98×10^7	11.47 ± 6.30	15.27 ± 8.46	0.314	0.255
1:30	9.92×10^6	9.47 ± 3.20	9.67 ± 3.18	0.157	0.577
1:90	3.31×10^6	4.47 ± 2.72	3.53 ± 2.70	0.119	0.672
1:270	1.10×10^6	2.00 ± 1.31	1.20 ± 1.21	−0.090	0.749
All data		6.85 ± 5.35	7.42 ± 7.21	0.411	0.001[b]

[a] Half leaves were inoculated separately with TEV-GFP, and the number of foci per half leaf was quantified. For no one dose was a significant correlation between half leaves observed.

[b] When the data from different doses were pooled, the partial correlation, with dose taken as a factor, was significant.

was therefore decided to measure the median time until onset of symptoms (ST_{50}) for high (1:10 virion dilution) and low (1:270 virion dilution) doses to rule out dose-dependent effects. The first symptom observed in most infected plants was vein clearing in the 5th true leaf, and all plants developed symptoms by 8 dpi. The Kaplan-Meier estimate for the mean time until onset of symptoms ± 1 standard error of the mean (SEM) was 5.47 ± 0.15 for the high dose and 5.66 ± 0.13 for the low dose, and the difference is nonsignificant (log rank test) ($\chi^2 = 0.924$; 1 df; $P = 0.336$). We therefore concluded that dose and N_e have no effect on the onset of symptoms in this experimental setup and that all infected plants eventually develop symptoms.

Effects of dose and N_e on viral accumulation. Next, it was considered whether there is an effect of dose on viral accumulation as measured by RT-qPCR assay. Viral accumulation increased significantly with dose (Fig. 3) (JT test; $P < 0.001$). A significant relationship between N_e and viral accumulation was also found (Fig. 4) (JT test; $P < 0.001$). However, viral accumulation was negatively affected only for small values of N_e (i.e., $N_e < 5$), and accumulation appeared to reach a plateau for larger N_e values. To test if this was the case, a geometric model of viral accumulation was fitted to the data (see Materials and Methods). Estimated model parameters show that for every unit increase in N_e, the increase in accumulation changes by a factor k of 0.564 ± 0.095 (mean estimate ± 1 SEM), which is significantly less than 1 (one-sample t test) ($t_{59} = 4.590$; $P < 0.001$) (Table 5). Hence, estimated model parameters also support the idea that accumulation is dependent on N_e and that the dependence is significantly below the linear expectation. This test result further reinforces the idea that this effect is manifest only when N_e is small.

N_e-dependent effects on accumulation are not a heritable trait of the virus population. There are a number of plausible reasons that the level of accumulation might be lower for small N_e values. TEV has a reasonably high mutation rate (34), and the fitness effects of many TEV mutations are deleterious (7). Therefore, if only a small number of TEV genomes start infection, there may be a reasonably high probability that all of the infecting genomes carry deleterious mutations and that these mutations result in less accumulation. For those plants infected with an N_e of 1, genetic variation in the population must be generated *de novo*. Therefore, less accumulation due to deleterious mutations in the viral genome should be heritable to a large extent. New plants were therefore infected with sap containing equal virion concentrations, calculated as genome equivalents by RT-qPCR, from the first replicate of the original experiment. Virus populations from those plants that gave the highest and lowest levels of accumulation were used. There were significant differences in accumulation when the three populations with the highest and lowest levels of accumulation were considered (nested analysis of variance [ANOVA]) (Table 6, experiment 0). We hypothesized that if accumulation is a heritable trait, the difference between these two populations would persist among their descendants. Although compensatory mutations or reversions could occur, they would not be expected in all replicates on such short time scales (i.e., two passages since the bottleneck where $N_e = 1$).

Two independent experiments were performed. In experiment 1, sap from each of the three plants which gave the highest and lowest levels of accumulation was used to infect three new plants, and accumulation was then determined by RT-qPCR. In experiment 2, sap from each of the two plants which gave the highest and lowest levels of accumulation was used to infect five new plants. There was no evidence for heritable differences in accumulation in both experiments (nested ANOVA) (Table 6). We can therefore conclude that the effect of small N_e values on viral accumulation is not necessarily explained by the presence of deleterious mutations in the inoculum. This conclusion is not at odds with previous

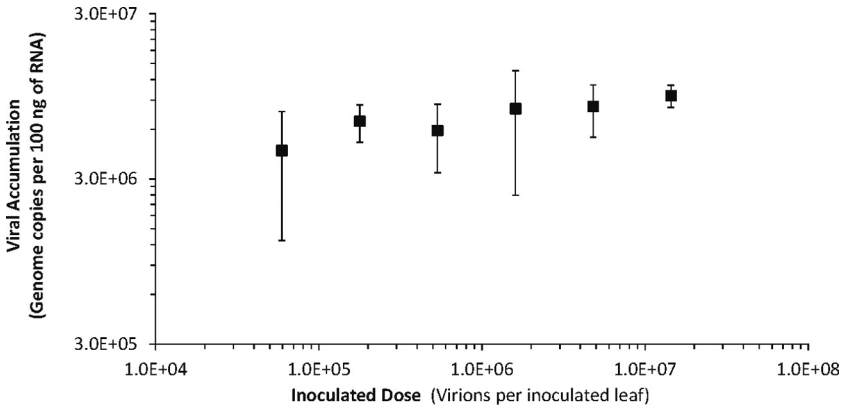

FIG 3 Effects of dose on viral accumulation at 6 dpi. The virion dose is plotted on the abscissa, and viral accumulation at 6 dpi (number of genome copies per 100 ng of total RNA extracted from plants) is plotted on the ordinate. Note that both scales are logarithmic. The mean accumulation ± standard deviation is given and appears to increase with dose. A Jonckheere-Terpstra test confirmed that there is a significant increase in accumulation with dose.

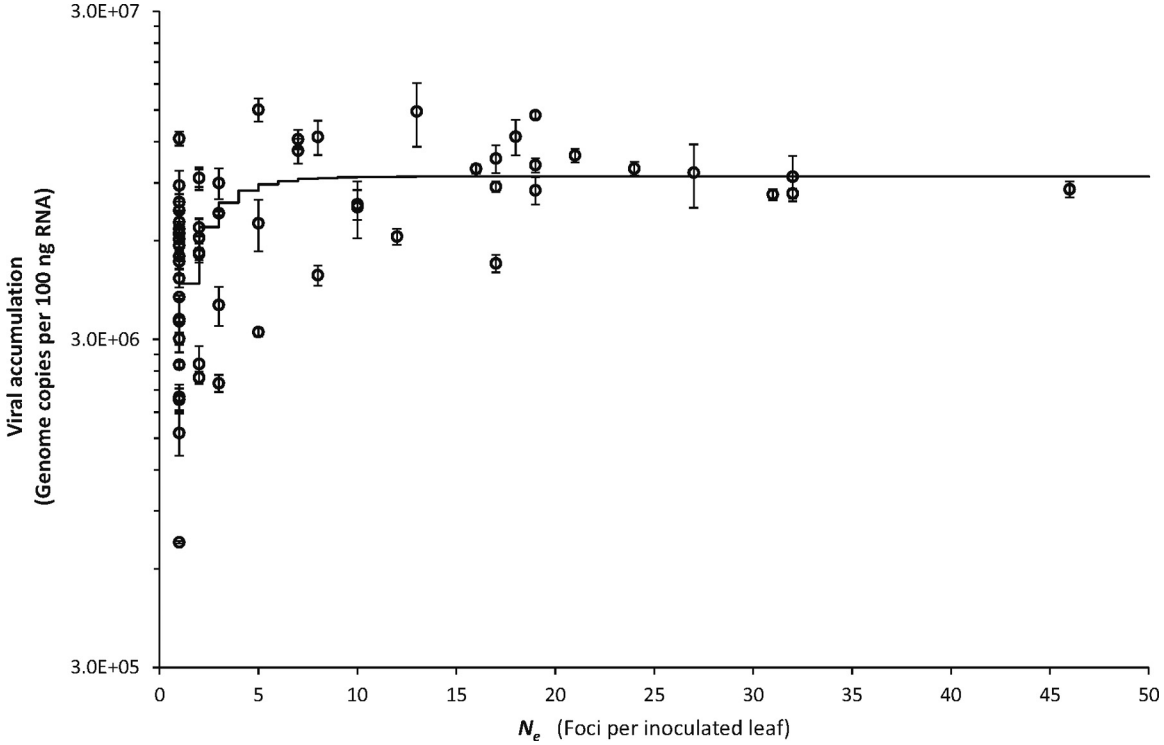

FIG 4 Effects of N_e on accumulation at 6 dpi. N_e is plotted on the abscissa, and viral accumulation at 6 dpi (number of genome copies per 100 ng of total RNA extracted from plants) is plotted on the ordinate. Circles represent measurements for individual plants; error bars show standard deviations. A Jonckheere-Terpstra test demonstrated that there is a significant increase of accumulation with N_e. The line depicts the fitted geometric model, which confirms that the increase of accumulation with N_e occurs only for small N_e values.

results on the distribution of mutational fitness effects, as these experiments considered within-host competitive fitness instead of accumulation (7). Virus genotypes can have identical accumulation while having marked differences in competitive within-host fitness (M. P. Zwart, J. A. Daròs, and S. F. Elena, unpublished data), suggesting that within-host fitness is more sensitive to mutational effects than viral accumulation.

***N_e*-dependent effects on accumulation are due to infection dynamics in the inoculated leaf.** A second possible explanation for N_e-dependent differences in accumulation is the infection process in the inoculated leaf. The infection process in the inoculated leaf is different from that in the systemically infected tissue. In the inoculated leaf, the foci of primary infection will typically expand only locally and along vascular tissue while exiting the leaf (Fig. 5). It is therefore likely that there is dose-dependent accumulation in the inoculated leaf at low doses when the inoculated leaf does not become saturated with primary infection foci. Moreover, because viral accumulation was measured early in infection, when the inoculated leaf (third true leaf) was the largest leaf, the contribution of accumulation of the inoculated leaf to accumulation in the entire plant may be considerable.

To test this possibility, plants were infected with either a high or low virion dose. Plants with an N_e of 1, as determined by microscopy at 3 dpi, were selected from the low-dose treatment group for further analysis, and plants with an N_e of >10 were selected from the high-dose treatment group. At 6 dpi, fluorescence in the inoculated leaf and the systemically infected tissue was observed, and the inoculated leaf and the remaining aerial tissue were then collected separately. Viral accumulation was then determined separately for the inoculated leaf and the rest of the plant. Whereas viral accumulation in the systemically infected tissue was not dependent on N_e (Tamhane's test; $P = 0.119$), viral accumulation in the inoculated leaf was clearly dependent on N_e (Tamhane's test; $P < 0.001$). There was a >5-fold N_e-dependent difference in accumulation in the inoculated leaf [mean accumulation ± standard deviation for an N_e value of 1, $(3.59 \pm 1.52) \times 10^6$; that for an N_e value of >10, $(2.05 \pm 0.58) \times 10^7$]. Thus, our hypothesis that differences in viral accumulation are due largely to the inoculated leaf was confirmed.

TABLE 5 Estimated parameters for geometric model of N_e-viral accumulation relationship[a]

Parameter	Estimate	SE	95% CI	
			Lower limit	Upper limit
A_0	5.816×10^5	1.229×10^6	-1.877×10^6	3.040×10^6
c	3.848×10^6	9.045×10^5	2.038×10^6	5.657×10^6
k	0.564	0.095	0.373	0.755

[a] Estimated model parameters for the fitting of a geometric model to N_e-viral accumulation data (see Materials and Methods). Key model parameters are c, which is positive, indicating that there is an increase of accumulation with N_e, and k, which is significantly less than 1, indicating that with each increment in N_e, the increase in viral accumulation becomes smaller.

***N_e*-dependent differences in viral accumulation when the inoculated leaf is removed.** As a further test of how N_e in the inoculated leaf affects accumulation in systemic tissue, plants were infected with high and low virion doses, and focus numbers were

TABLE 6 Results of nested ANOVAs for analysis of viral accumulation in 3 experiments[a]

Expt	Source of variation	SS	df	MS	*F*	*P*	% of variance explained by model
0	Class (high or low)	2.809	1	2.809	35.52	0.004	84.35 ± 13.77
	Lineage within class	0.316	4	0.079	57.93	<0.001	14.86 ± 0.17
	Error	0.016	12	0.001			0.78 ± 0.00
1	Class (high or low)	0.094	1	0.094	4.56	0.100	0.98 ± 0.00
	Lineage within class	0.082	4	0.021	0.76	0.571	0.00 ± 0.00
	Replicate within lineage within class	0.325	12	0.027	20.25	<0.001	98.8 ± 0.11
	Error	0.048	36	0.001			0.1 ± 0.00
2	Class (High or Low)	0.166	1	0.166	5.88	0.136	2.58 ± 0.04
	Lineage within class	0.057	2	0.028	0.40	0.678	0.00 ± 0.00
	Replicate within lineage within class	1.137	16	0.071	16.10	<0.001	95.38 ± 0.23
	Error	0.177	40	0.004			2.04 ± 0.00

[a] Viral accumulation in three separate experiments was analyzed with nested ANOVAs. Experiment 0 was the analysis of the 3 plants with an N_e of 1 and the highest or lowest level of accumulation in the original accumulation experiment (Fig. 4). Experiments 1 and 2 were the first and second experiments to determine the heritability of accumulation, respectively. SS, sum of squares; MS, mean square. The percentage of variance explained by the model was estimated by a maximum likelihood-based variance component analysis in SPSS, and the asymptotic covariance is given as an indication of estimate error.

confirmed at 3 dpi. As soon as virus-induced fluorescence was visible in the systemically infected tissue of all plants in the experiment (5 dpi), the inoculated leaf was removed. The remaining aerial plant tissue was collected at 6 dpi, and viral accumulation was determined (Fig. 6). A significant effect of N_e on accumulation was found (*t* test on $\log_{10}$-transformed accumulation) ($t_{14} = 2.802$; $P = 0.014$). Nevertheless, there was only a 1.5-fold difference in accumulation [mean accumulation ± standard deviation for an N_e value of 1, $(1.14 \pm 0.40) \times 10^7$; that for an N_e value of >10, $(1.73 \pm 0.29) \times 10^7$]. The differences in accumulation for large and small N_e values were therefore much smaller than the differences observed in the inoculated leaf at 6 dpi.

Why does removal of the inoculated leaf at 5 dpi result in less viral accumulation in plants with a small N_e, whereas there are no N_e-dependent differences when the inoculated leaf is not removed? We think that this effect occurs because the flux of virions egressing from the inoculated leaf at any time point depends on the number of primary infection foci, while the systemic tissue of the plant can eventually be largely saturated by the virion production of even a single focus. Note that this explanation does not

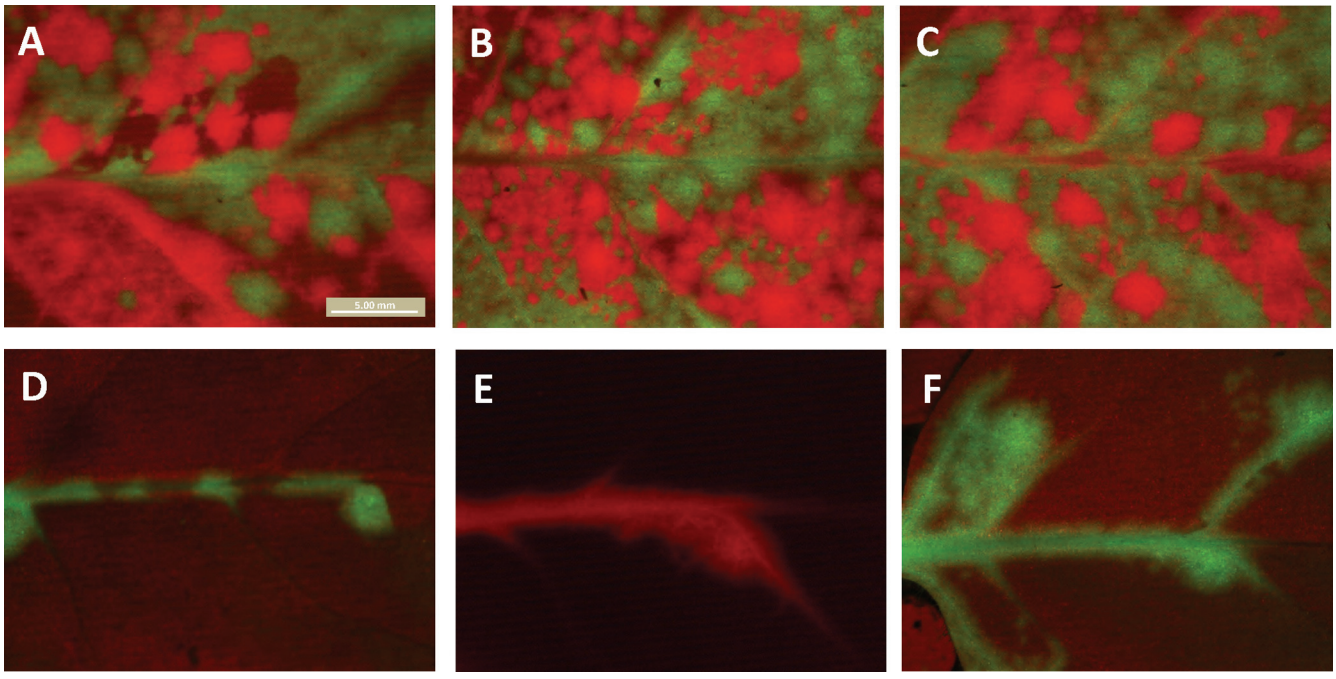

FIG 5 Fluorescence in the inoculated leaf at high and low doses. GFP and mCherry fluorescence is shown for inoculated *N. tabacum* leaves at 6 dpi. For panels A to C, a high virion dose was given (1.44×10^7), whereas for panels D to F a low virion dose was given (5.34×10^5), and plants with a single focus of primary infection at day 3 were selected. RT-qPCR also demonstrated significantly less accumulation in the inoculated leaves of plants infected at only a single focus. Note the variation in the amount of fluorescence at low doses (D to F). In some cases, only the focus of primary infection and a faint trail along the vascular tissue are present (D), whereas in other cases the virus did achieve limited expansion into the inoculated leaf (F).

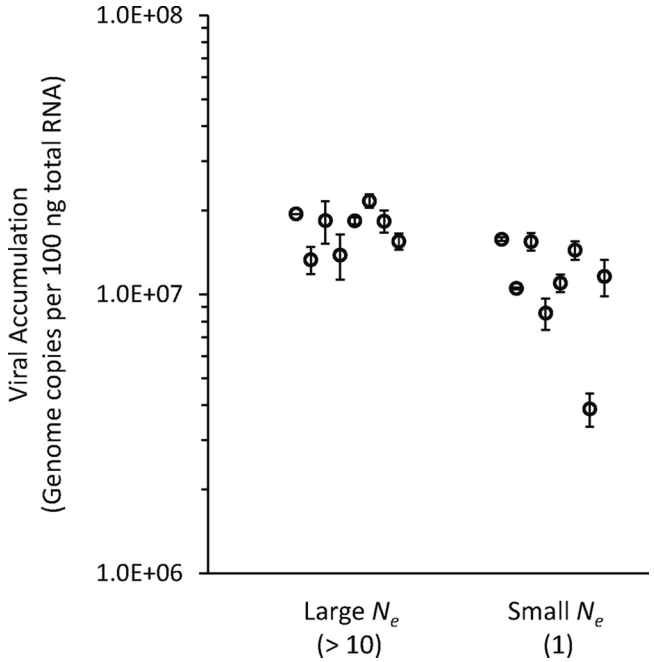

FIG 6 Effects of N_e on accumulation when the inoculated leaf is removed. Viral accumulation at 6 dpi is given for plants infected with a large or small N_e. The inoculated leaf was removed at 5 dpi, when all infected plants in the experiment had shown systemic fluorescence. Errors bars represent standard deviations.

imply a high multiplicity of infection (MOI) in systemically infected tissue, as mechanisms regulating MOI can act at the cellular level (e.g., coinfection exclusion). This idea would result in a small time window in which there are N_e-dependent effects on systemic accumulation, which all but vanish by 6 dpi. Moreover, the time at which individual primary infection foci start contributing to the flux of virions is likely to be subject to stochastic effects. These effects might come about due to the proximity of the initial infected epidermal cell to vascular bundles, in particular the number of mesophyll cells that must be traversed by means of cell-to-cell movement before phloem can be accessed. When N_e is large, not only are there more foci, but some of them are more likely to be situated fortuitously with respect to phloem in the inoculated leaf than the case when N_e is small. This mechanism may also explain why there is greater variation in viral accumulation at 6 dpi when N_e is small (Fig. 4 and 6). In summary, although systemic accumulation at 6 dpi appears to be N_e independent, these results show that there are N_e-dependent effects at earlier time points. We found in a related experimental study that N_e-dependent effects on systemic infection may be stronger if the inoculated leaf is removed earlier during infection (N. Tromas, G. Lafforgue, S. F. Elena, and M. P. Zwart, unpublished data).

***N*$_e$-dependent effects on accumulation are transient.** N_e-dependent effects on accumulation at 6 dpi are due to the level of infection in the inoculated leaf. At earlier time points in infection, these data suggest that there may also be N_e-dependent accumulation in systemic tissue (Fig. 6). We therefore hypothesized that the effect on accumulation in the whole plant should be transient. As the plant grows and infection expands, the inoculated leaf should contribute less to viral accumulation in all tissues, and its contribution eventually will become negligible. We speculate, moreover, that given enough time the number of virions egressing from the inoculated leaf will be sufficient, in combination with secondary infections, to saturate the systemic tissues irrespective of N_e. A time course experiment was therefore performed, with a

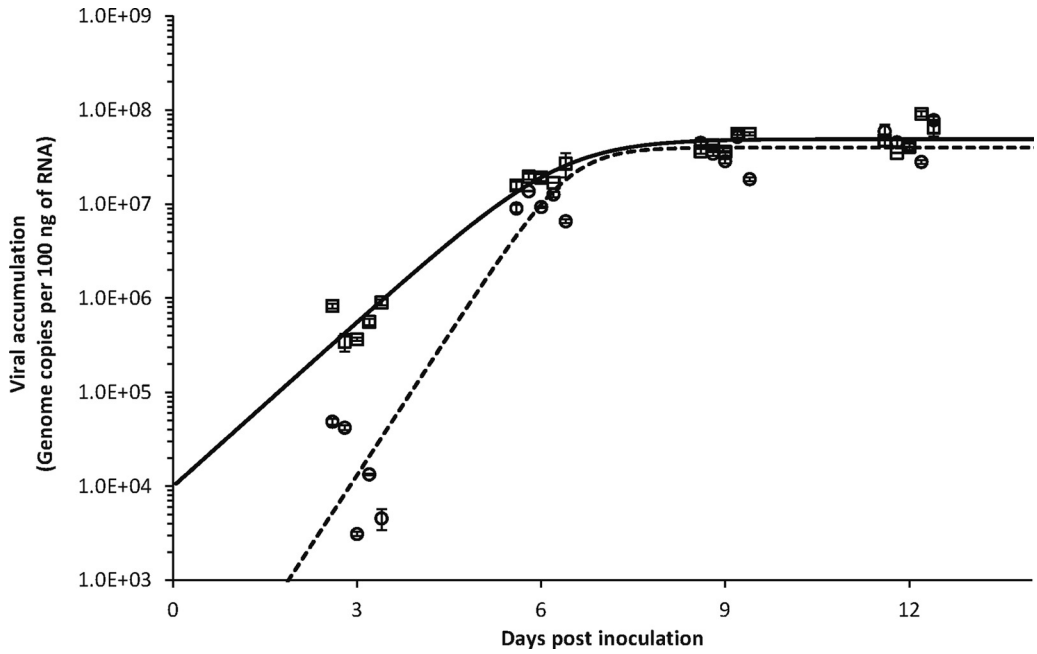

FIG 7 Time course experiment on the effects of N_e on accumulation. The time of collection is plotted on the abscissa, and viral accumulation (number of genome copies per 100 ng of total RNA extracted from plants) is plotted on the ordinate. Circles represent measurements for individual plants (error bars show standard deviations) from the low-dose treatment group (1:270 virion dilution; $N_e = 2.05 \pm 1.28$), whereas squares represent plants from the high-dose treatment group (1:10 virion dilution; $N_e = 23.30 \pm 10.57$). Lines represent a logistic model fitted to the high-dose (solid line) and low-dose (dotted line) data. There were effects of N_e on accumulation only at low doses, whereas similar levels of accumulation were measured at high doses.

TABLE 7 Estimated parameters for logistic model of viral accumulation over time[a]

Dose	N_e	Parameter	Estimate	SE	95% CI	
					Lower limit	Upper limit
Low	2.05 ± 1.28	n_0	13.11	9.82	−7.60	33.82
		r_0	2.303	0.174	1.936	2.669
		κ	3.988×10^7	8.768×10^6	2.138×10^7	5.838×10^7
High	22.30 ± 10.57	n_0	9,928	3,857	1,792	18,066
		r_0	1.344	0.098	1.138	1.550
		κ	4.905×10^7	5.226×10^6	3.802×10^7	6.008×10^7

[a] Estimated model parameters for the fitting of a logistic model to accumulation data over time for high (1:10 virion dilution) and low (1:270 dilution) doses. N_e values are mean estimates ± standard deviations obtained by counting the number of foci of primary infection on day 3. Estimates of κ, the carrying capacity, are similar, and 95% confidence intervals (CIs) overlap. Estimates of n_0 and r_0 also differ, as attested by nonoverlapping 95% CIs. For n_0, this difference (~738-fold) could be expected, and the low dose gives a lower parameter estimate. On the other hand, from a quantitative perspective, the difference in n_0 estimates does not match the difference in N_e (~10.9-fold) or dose (27-fold). Different estimates of r_0 occur because at high doses the systemic population experiences less growth relative to the initial population in the inoculated leaf than for low doses, and they probably do not reflect differences in the basic rate of viral replication.

setup identical to that in the first experiment described in this study. However, plants were infected only with a high (1:10 virion dilution) or low (1:270 virion dilution) dose. After the number of foci of primary infection was quantified at 3 dpi, plants were randomly assigned to be collected and stored at 3, 6, 9, and 12 dpi. Fluorescence and symptomatology were recorded at all times of collection for all available plants. In this experiment, there was no effect of dose on the onset of symptoms (log rank test) ($\chi^2 = 0.228$; 1 df; $P = 0.633$), confirming previous observations. Accumulation was measured by RT-qPCR for whole plants collected at different time points (Fig. 7), and a logistic model was fit to the data (see Materials and Methods). There were significant differences only at days 3 (Mann-Whitney U test; $P = 0.008$) and 6 ($P = 0.008$), but not later on (for day 9, $P = 0.175$; for day 12, $P = 0.841$). Fitting of the logistic model rendered similar estimates of κ (the carrying capacity) for both treatments (Table 7). These similar estimates further confirm that N_e-dependent effects on accumulation are transitory, as virus accumulation saturates at the same level regardless of N_e.

Concluding remarks. The results reported here demonstrate a manner in which N_e can affect the outcome of the infection process, in particular virus accumulation. Although this effect was demonstrated by means of mechanical inoculation, a similar effect could conceivably occur during infections initiated by vector-borne transmission (37). The number of feeding or probing events by viruliferous vectors or, alternatively, the density of viruliferous vectors could lead to differences in accumulation due to differences in the number of foci of primary infection, thereby contributing significantly to overall accumulation. On the other hand, the effect of N_e on accumulation was transitory, as it was observed only before 9 dpi. Moreover, N_e had no effect on accumulation at 6 dpi for most observed values (N_e values of ~5 to 50), and the onset of symptoms was independent of N_e. As a first approximation, ignoring N_e in models of infection or epidemiology that do not consider mixed-genotype infections therefore does not seem unreasonable for this model system. However, at low doses, N_e can have transient effects on viral accumulation, and incorporating this mechanism into models may lead to better insight into the infection and epidemiology of plant viruses.

A practical consideration also arises from the work presented here. For experiments comparing the accumulation of different genotypes in this model system, dose affects accumulation only if N_e values in individual plants drop below ~5, and this effect is due mainly to infection dynamics in the inoculated leaf. To avoid N_e-induced effects in experiments comparing accumulation of different viral genotypes, there are three possible tactics: (i) measuring accumulation only in the systemically infected tissue (a common laboratory practice), (ii) use of high doses, and (iii) measuring accumulation late in infection (i.e., at least 9 dpi for this system), when the contribution of the inoculated leaf to total inoculation is negligible and the systemic tissue has probably been saturated with virions from the inoculated leaf and from secondary infections in systemic tissue. The exact threshold value for N_e-induced effects (~5) probably depends on the exact experimental conditions used (e.g., size of the inoculated leaf and temperature) and should therefore not be seen as an absolute value.

ACKNOWLEDGMENTS

We thank Francisca de la Iglesia for technical assistance and three anonymous reviewers for their constructive comments.

This research was supported by Spanish Ministerio de Economía y Competitividad grant BFU2009-06993 to S.F.E. and grants BIO2008-01986 and BIO2011-26741 to J.-A.D. M.P.Z. was supported by a Rubicon grant from the Netherlands Organization for Scientific Research (www.nwo.nl) and the Juan de la Cierva Program of the Spanish Ministerio de Economía y Competitividad (JCI-2011-10379).

REFERENCES

1. **Ali A, et al.** 2006. Analysis of genetic bottlenecks during horizontal transmission of *Cucumber mosaic virus*. J. Virol. **80**:8345–8350.
2. **Bald JG.** 1937. The use of numbers of infections for comparing the concentration of plant virus suspensions: dilution experiments with purified suspensions. Ann. Appl. Biol. **24**:33–55.
3. **Bedhomme S, Lafforgue G, Elena SF.** 2012. Multihost experimental evolution of a plant RNA virus reveals local adaptation and host-specific mutations. Mol. Biol. Evol. **29**:1481–1492.
4. **Ben Ami F, Regoes RR, Ebert D.** 2008. A quantitative test of the relationship between parasite dose and infection probability across different host-parasite combinations. Proc. Biol. Sci. **275**:853–859.
5. **Betancourt M, Fereres A, Fraile A, García-Arenal F.** 2008. Estimation of the effective number of founders that initiate an infection after aphid transmission of a multipartite plant virus. J. Virol. **82**:12416–12421.
6. **Carrasco P, Daròs JA, Agudelo-Romero P, Elena SF.** 2007. A real-time RT-PCR assay for quantifying the fitness of *Tobacco etch virus* in competition experiments. J. Virol. Methods **139**:181–188.
7. **Carrasco P, de la Iglesia F, Elena SF.** 2007. Distribution of fitness and virulence effects caused by single-nucleotide substitutions in *Tobacco etch virus*. J. Virol. **81**:12979–12984.
8. **Elena SF, et al.** 2011. The evolutionary genetics of emerging plant RNA viruses. Mol. Plant Microbe Interact. **24**:287–293.

9. **French R, Stenger DC.** 2003. Evolution of *Wheat streak mosaic virus*: dynamics of population growth within plants may explain limited variation. Annu. Rev. Phytopathol. **41**:199–214.
10. **Froissart R, et al.** 2005. Recombination every day: abundant recombination in a virus during a single multi-cellular host infection. PLoS Biol. **3**:e89. doi:10.1371/journal.pbio.0030089.
11. **Furumoto WA, Mickey R.** 1967. A mathematical model for infectivity-dilution curve of *Tobacco mosaic virus*—experimental tests. Virology **32**: 224–233.
12. **Gómez P, Sempere RN, Elena SF, Aranda MA.** 2009. Mixed infections of *Pepino mosaic virus* strains modulate the evolutionary dynamics of this emergent virus. J. Virol. **83**:12378–12387.
13. **Grenfell BT, et al.** 2004. Unifying the epidemiological and evolutionary dynamics of pathogens. Science **303**:327–332.
14. **Hall JS, French R, Hein GL, Morris TJ, Stenger DC.** 2001. Three distinct mechanisms facilitate genetic isolation of sympatric *Wheat streak mosaic virus* lineages. Virology **282**:230–236.
15. **Hall JS, French R, Morris TJ, Stenger DC.** 2001. Structure and temporal dynamics of populations within *Wheat streak mosaic virus* isolates. J. Virol. **75**:10231–10243.
16. **Hammond AM, Hardy TN.** 1988. Quality of diseased plants as hosts for insects, p 657–672. *In* Heinrichs EA (ed), Plant stress-insect interactions. Wiley, New York, NY.
17. **Jeger MJ.** 1982. The relation between total, infectious and post-infectious plant diseased plant tissue. Phytopathology **72**:1185–1189.
18. **Keeling MJ, Rohani P.** 2008. Modeling infectious diseases in humans and animals. Princeton University Press, Princeton, NJ.
19. **Kermack WO, McKendrick AG.** 1927. A contribution to the mathematical theory of epidemics. Proc. R. Soc. A **115**:700–721.
20. **Kleczkowski A.** 1950. Interpreting relationships between the concentrations of plant viruses and numbers of local lesions. J. Gen. Microbiol. **4**:53–69.
21. **Lalić J, Cuevas JM, Elena SF.** 2011. Effect of host species on the distribution of mutational fitness effects for an RNA virus. PLoS Genet. **7**:e1002378. doi:10.1371/journal.pgen.1002378.
22. **Li H, Roossinck MJ.** 2004. Genetic bottlenecks reduce population variation in an experimental RNA virus population. J. Virol. **78**:10582–10587.
23. **Mideo N, Alizon S, Day T.** 2008. Linking within- and between-host dynamics in the evolutionary epidemiology of infectious diseases. Trends Ecol. Evol. **23**:511–517.
24. **Moury B, Fabre F, Senoussi R.** 2007. Estimation of the number of virus particles transmitted by an insect vector. Proc. Natl. Acad. Sci. U. S. A. **104**:17891–17896.
25. **Moya A, Elena SF, Bracho A, Miralles R, Barrio E.** 2000. The evolution of RNA viruses: a population genetics view. Proc. Natl. Acad. Sci. U. S. A. **97**:6967–6973.
26. **Ng JC, Tian T, Falk BW.** 2004. Quantitative parameters determining whitefly (*Bemisia tabaci*) transmission of *Lettuce infectious yellows virus* and an engineered defective RNA. J. Gen. Virol. **85**:2697–2707.
27. **Read AF, Taylor LH.** 2001. The ecology of genetically diverse infections. Science **292**:1099–1102.
28. **Regoes RR, Hottinger JW, Sygnarski L, Ebert D.** 2003. The infection rate of *Daphnia magna* by *Pasteuria ramosa* conforms with the mass-action principle. Epidemiol. Infect. **131**:957–966.
29. **Sacristán S, Malpica JM, Fraile A, García-Arenal F.** 2003. Estimation of population bottlenecks during systemic movement of *Tobacco mosaic virus* in tobacco plants. J. Virol. **77**:9906–9911.
30. **Sedarati F, Javier RT, Stevens JG.** 1988. Pathogenesis of a lethal mixed infection in mice with two nonneuroinvasive herpes simplex virus strains. J. Virol. **62**:3037–3039.
31. **Simón O, Williams T, Caballero P, López-Ferber M.** 2006. Dynamics of deletion genotypes in an experimental insect virus population. Proc. Biol. Sci. **273**:783–790.
32. **Stout MS, Thaler JS, Thoma BPHJ.** 2006. Plant-mediated interactions between pathogenic microorganisms and herbivorous arthropods. Annu. Rev. Entomol. **51**:663–689.
33. **Syller J.** 2012. Facilitative and antagonistic interactions between plant viruses in mixed infections. Mol. Plant Pathol. **13**:204–216.
34. **Tromas N, Elena SF.** 2010. The rate and spectrum of spontaneous mutations in a plant RNA virus. Genetics **185**:983–989.
35. **van der Plank JE.** 1965. Dynamics of epidemics of plant disease. Science **147**:120–124.
36. **van der Werf W, Hemerik L, Vlak JM, Zwart MP.** 2011. Heterogeneous host susceptibility enhances prevalence of mixed-genotype micro-parasite infections. PLoS Comput. Biol. **7**:e1002097. doi:10.1371/journal.pcbi.1002097.
37. **Watson MA.** 1972. Transmission of plant viruses by aphids, p 131–167. *In* Kado CI, Agrawal HO (ed), Principles and techniques in plant virology. Van Nostrand Reinhold Co., New York, NY.
38. **Wright S.** 1931. Evolution in Mendelian populations. Genetics **16**:97–159.
39. **Zwart MP, Daròs JA, Elena SF.** 2011. One is enough: *in vivo* effective population size is dose-dependent for a plant RNA virus. PLoS Pathog. **7**:e1002122. doi:10.1371/journal.ppat.1002122.
40. **Zwart MP, et al.** 2009. An experimental test of the independent action hypothesis in virus-insect pathosystems. Proc. Biol. Sci. **276**:2233–2242.